DEVELOPMENT OF A HIGH RESOLUTION CHEMICALLY REACTIVE NEAR-FIELD DISPERSION MODEL FOR ASSESSING THE IMPACT OF MOTOR VEHICLE EMISSIONS. PART 1: MODEL DESCRIPTION AND VALIDATION.

William Lilley[1] and Martin Cope[2]
[1] CSIRO, Division of Energy Technology, PO Box 330, Newcastle, NSW 2300.
[2] CSIRO, Division of Atmospheric Research, PMB 1 Aspendale Vic 3195.

Abstract

The Lagrangian Wall Model (LWM) is a fine-scale dispersion model which has been developed to assess the near-field impact of line, area and point sources, which themselves may be imbedded within a larger scale concentration field. The model consists of a two-dimensional wall of cells which moves in very high resolution spatial steps (typically 10 m) through a region of interest at a speed governed by the vertically averaged wind. The wind fields, the initial concentrations across the 'wall' (specified upwind of the region of interest), and boundary conditions at the edges of the wall, are either prescribed from observations or derived from The Air Pollution Model. As the wall is advected through the region, the LWM's fine resolution is able to resolve emissions from such small-scale features as roads, industrial point sources and tunnel stack vents. The diffusion-chemical transformation module utilises a dynamic chemistry compiler capable of interpreting a text file description of any chemically reactive scheme, and is currently defined for a simple tracer scheme, and for simple and comprehensive photochemical transformation schemes.

The ability to combine emission estimates from a power-based motor vehicle emissions model with the LWM dispersion and chemical transformation capabilities has greatly enhanced our capacity for modelling emissions from roads. The incorporation of the power based emission model allows a dynamic representation of emissions from motor vehicles by accounting for driving behaviour associated with different road types, including gradients and traffic-light intersections.

This paper discusses the development of the LWM, and summarises the outcomes of a verification study using the Caltrans Highway 99 tracer dispersion data set. Model results are compared with those obtained from Caline-4.

Keywords: Lagrangian, near-road, Caline, motor vehicle, air pollution.

1. Introduction

A number of mathematical models have been developed to predict the dispersion of pollutants from roadways. The majority of these models are based on Gaussian formulations and are used primarily to predict the dispersal of inert tracers. Commonly used Gaussian models include the Hiway series, Caline series, GM model, GFLSM and ISCST-2 (see references in the review of Sharma and Khare 2001). More complex formulations include Roadway-2 (Rao, 2002) which solves a 2D scalar conservation equation and UCD 2001 which implements a Huang similarity solution (Held et al., 2003). It is usual for the contemporary versions of these models to provide a treatment of vehicle induced wakes and often to also include an estimate of the effect of enhanced buoyancy from the vehicle exhausts. Of the models listed, only Caline-4 and Roadway-2 incorporate the effects of chemistry and in both cases consist of a simple NO-NO_2-O_3 mechanism.

Given that Caline-4 is one of the most commonly used models in Australia, we have elected to use it as a benchmark when comparing the Lagrangian

Wall Model with data from the Caltrans Highway 99 tracer experiment (Benson, 1989).

All roadway dispersion models require emissions to be input in the form of line sources with common resources including outputs from emission models based upon an emission per vehicle kilometre travelled (VKT) approach with some including adjustment factors for vehicle speed. Whilst the LWM is capable of utilising these emission estimates, it was primarily built to accommodate the power based profiles provided by the CVEM model developed by CSIRO (Nguyen et al., 2000). Whilst the effect of vehicle emission rate is of critical importance, this paper is restricted to the consideration of the development of the LWM dispersion model and the outcomes of a preliminary validation for an inert tracer, using the Caltrans Highway 99 experiment. In a companion paper we provide an example of an application in which the LWM is used to assess the air quality impacts of implementing various intelligent transport systems to improve traffic flow in Sydney.

2. Model description

2.1. General

The LWM system consists of a GUI based pre-processor, a diffusion-chemical solver and a GUI based post-processing facility. The pre-processor defines the size of the wall and contains routines to calculate the trajectory path, assign initial concentrations, boundary concentrations and emissions from area, point and line sources. The diffusion-chemical solver utilises a trajectory file generated by the pre-processor to integrate a predefined chemical system using a K-theory approximation of the two dimensional diffusion equation (equation 5). Finally the post processing facility allows concentration profiles to be visualised and interrogated in three dimensions. The complete system is Windows® based and utilises the Microsoft™ DirectX® graphics engine.

2.2. Trajectory calculations

A trajectory is defined as the path followed by a vertical two dimensional wall of cells as it is advected by a prescribed (i.e. from observations) or TAPM (Hurley, 2002) derived wind field (Figure 1). The trajectory is generated by integrating an Euler equation forwards and backwards in time from a user prescribed 'anchor point'. By default the anchor time is set at the mid point of the meteorological timestep (i.e. at the half hour). Initial and final integration times are by default set to the beginning and end of the meteorological timestep, but can be set any range within the bounds of the meteorological input data. While studies of vehicle emissions are not likely to be interpolated outside the selected meteorological timestep, this functionality allows longer time scale studies to be conducted. For instance the LWM is currently being used to estimate the formation rates of sulphate and nitrate in a power station plume travelling up to 150 km from the Hunter, Central Coast or Western Sydney regions into the Sydney airshed.

The size of the wall is determined by the number of rows and columns. The column width is user specified and is defined to be constant across the wall. The height of each row is independent and adjustable allowing a vertically staggered grid with highest resolution near to the ground.

Meteorology can be prescribed from observations or derived from TAPM output. When using TAPM outputs the layer average wind is specified between the ground (TAPM layer 1) and the mixing height by default. In addition the modeller can derive meteorology from alternate TAPM layers, which may be of use in near field applications of ground level sources. The size of each advection step is prescribed by the modeller in either a constant distance or constant timestep mode. Default settings are for a distance step of 10 m. The trajectory position of the wall is calculated at each step using an iterative predictor-corrector scheme until the change is less than 0.1% of the defined distance or time. Meteorology can be prescribed as constant in time or allowed to vary in time and space using an interpolation from the prescribed or TAPM generated hourly average fields.

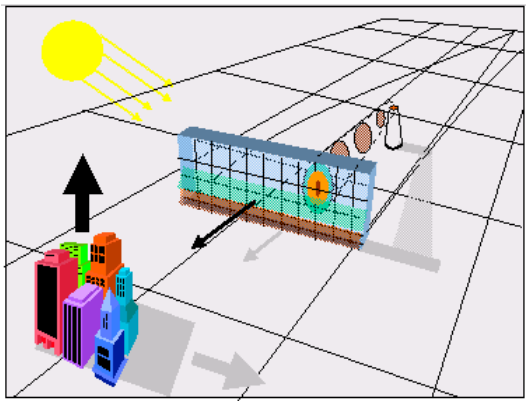

Figure 1. Schematic representation of LWM

2.3. Initial conditions

To solve chemistry, initial concentrations, boundary concentrations and sources must be prescribed. Initial and boundary concentrations can be either prescribed as constant above and below the mixing height or interpolated to each cell from the three dimensional concentration fields of TAPM. The chemical transformation module utilises a dynamic chemistry compiler capable of interpreting a text file

description of user-defined chemical mechanism. Currently the model is defined with a tracer (up to 4), GRS (Azzi, 1992) and a Carbon Bond, CB99, (Alderman, 1999) mechanism. To operate with complex photochemistry eg CB99 using the current version of TAPM (v. 2.5), a VOC speciation file and a reactivity coefficient is required for each TAPM source type (biogenic, area, point, wood heater, petrol, petrol evaporative, diesel and LPG). Ambient concentrations of smog reactivity as output by TAPM are treated similarly using prescribed speciation profiles and a reactivity coefficient.

A source emission rate is determined for each cell per step and is a total of the contribution from all area, point and line sources intercepted by the wall during the current timestep. Area and point source files are prescribed in standard TAPM format and have GUI definable scale factors for each pollutant and on/off switches for each source, thereby easily allowing source sensitivity studies to be undertaken. Plume rise for point sources is calculated in accordance with Briggs (1975). The initial plume spread can be defined as Gaussian or Top Hat. Surface area sources may be injected into one- or more of the near-surface rows in the wall.

Line sources are also scalable and are defined in accordance with outputs from the CVEM model. CVEM outputs include fuel consumption, CO_2 and pollutant emission rates for petrol, petrol evaporative, diesel and LPG vehicles and include average tailpipe height, average vehicle speed and traffic volumes for each vehicle source on each road link. An option is available to allow TAPM area based vehicle sources to be used in conjunction with the CVEM estimates. Typically this option is employed when modelling residential roadway emissions in a gridded format whilst handling the major roads via the CVEM.

Initial mixing for the line sources can be prescribed by placing emissions into specified layers of the wall or using a Caline-4 or modified Caline-4 based algorithm. The Caline-4 algorithm calculates an initial vertical dispersion coefficient; σ_{zi} within a mixing zone defined as the width of the roadway plus 3 metres each side. The coefficient is calculated using a residence time which increases as the ambient wind speed decreases (equation 1). The algorithm is implemented in LWM by releasing emissions at the tailpipe height for each vehicle source and apportioning mass into appropriate layers assuming total reflection from the ground.

$$\sigma_{zi} = 1.5 + TR/10 \qquad 1)$$

where

$$TR = 0.5w/\overline{U}.\sin(\theta), \quad \theta \geq 45^\circ$$
$$TR = 0.5w/\overline{U}.\sin(45), \quad \theta < 45^\circ \qquad 2)$$

and, w = road width plus 3m each side

$\overline{U}$ = ambient wind speed.

θ = wind-road angle (90° = crosswind)

In the modified version (equation 3) an adjustment factor is added to allow σ_{zi} to marginally decrease as the wind approaches a perpendicular direction to the roadway, and to increase for parallel winds. This adjustment is based on the assertion that the vertical dispersion of emissions in the case of parallel winds is further enhanced by trailing vehicles than those emitted into ambient cross winds.

$$\sigma_{zi} = (0.85 + AF \times 1.5) + TR/(10 \times AF) \qquad 3)$$

where, AF = Max[0.1,1-Sin(θ)]

2.4. Diffusion coefficents

A number of options are available for the determination of the horizontal (K_h), and vertical (K_z), dispersion coefficients used in the chemical transformation model. The LWM solves the two dimensional atmospheric diffusion equation using a K-Theory approximation to the turbulent flux of concentration of a species, C_i.

To overcome limitations associated with the use of a constant diffusivity, a number of options are available to define a modified diffusivity derived from a Gaussian sigma (σ) value according to;

$$K_h = \overline{u}.\sigma_y^2/2x$$
$$K_z = \overline{u}.\sigma_z^2/2x \qquad 4)$$

where, x = downwind distance.

Whilst a K-theory solution using constant diffusivities generates a Gaussian solution, the σ values used in Gaussian modelling are empirically based, allowing for the limiting behaviour of statistical theory to be realised, i.e. $\sigma \approx t$ as $t \to 0$ and $\sigma \approx t^{1/2}$ as $t \to \infty$ (Seinfeld and Pandis, 1998). To implement the Gaussian solution, the downwind distance is reset each time a roadway source is encountered within a column of the wall. The distance from the last roadway source in each column is then incrementally increased as the trajectory proceeds and used to determine K_h and/or K_z. A selectable distance is used to determine diffusivities prior to an encounter with a roadway source. For acute wind-road angles less than 15 degrees, the distance is taken as the maximum of the incremental distance or 100 m.

Horizontal diffusivities, K_h, are determined from a choice of (Seinfeld and Pandis, 1998);

- Surface similarity theory, or
- A Gaussian, σ_y, value based on horizontal wind fluctuations, σ_θ, or
- A Gaussian, σ_y, value based on a Pasquill-Gifford formulation.

The method employing wind fluctuations is advantageous in that it implicitly accounts for the effect of averaging time on plume meander through the definition of σ_θ. All other methods using K or σ based values imply an averaging period of 15 minutes or more.

Vertical diffusivities, K_z, are given from a choice of;

- A Hysplit algorithm (Draxler and Hess, 2004), or
- A Hysplit algorithm using a modified σ_z value incorporating buoyancy enhancements (Benson, 1989), within the surface layer, which is defined as the maximum of $0.1Z_i$ or $2\sigma_{zi}$, where Z_i is the mixing height.

Buoyancy enhancements are derived from heat fluxes in accordance with Caline-4 parameterisations (Benson, 1989) when fuel consumption rates are unknown or derived from fuel consumption estimates when provided.

2.5. Chemical-diffusion Solver

The chemical transformation module, which is currently configured for a tracer (up to 4), GRS and CB99 mechanisms, integrates the two dimensional atmospheric diffusion equation (equation 5) allowing for diffusion, deposition and chemical transformation using a K-theory approximation;

$$\frac{\partial \langle C_i \rangle}{\partial t} = \frac{\partial}{\partial x_j}\left(K_{jj} \frac{\partial \langle C_i \rangle}{\partial x_j} \right) + Ri + S\mathrm{i} \qquad 5)$$

where, t is time, C_i, S_i and R_i are the concentration, source rate and removal rate of the i^{th} species respectively.

The diffusion component is represented as an equivalent chemical formation or loss rate for each cell, i.e.

$$\frac{\partial C_i}{\partial t} = F_i - L_i C_i \qquad 6)$$

Taking a non boundary cell in the vertical direction as an example and treating each cell as a control volume, the formation and loss terms can be expressed as;

$$F = \left(\frac{K_N C_N}{\delta z_N \Delta z} \right) + \left(\frac{K_S C_S}{\delta z_S \Delta z} \right)$$
$$LC = -\left(\frac{K_N C_P}{\delta z_N \Delta z} \right) - \left(\frac{K_S C_P}{\delta z_S \Delta z} \right) \qquad 7)$$

Here the rates are derived from the gradient of concentration between the midpoints of the centre cell, P, and adjacent rows, subscripts N and S. Horizontal diffusion is treated similarly using concentrations in adjacent columns.

Dry deposition is accounted for by including in the surface layer (row 1) a deposition velocity based upon a total resistance analogy (Seinfeld and Pandis, 1998). The deposition velocity is calculated from land use, roughness and appropriate surface scaling factors either prescribed or derived from TAPM.

The set of coupled nonlinear ordinary differential equations described by equation 6 and defined by the dynamic chemistry compiler, are solved using a modified version of a hybrid predictor-corrector algorithm originally applied in the CIT airshed model (McRae et al., 1982). The solution procedure uses a combination of semi-implicit and explicit techniques, selected by dividing the system into three stiff and non-stiff solution categories, based upon speed of the reaction. A variable time step, is bounded by a Courant number restriction.

3. Caltrans 99 Validation

3.1. Description of Caltrans 99 experiment

The Caltrans 99 data set is provided in Appendix C of the Caline-4 manual. The experiment was performed in Sacramento, California during the winter of 1981-1982. The procedure involved releases of a tracer gas (SF_6) from eight vehicles continuously travelling along a 4 km section of Highway 99. The roadway consists of two lanes in each direction separated by a 14 metre wide median strip and runs in a NW direction (N 40º13' W). Primary bag samples were taken 1.05 km from the southern end of the roadway at distances of 0, 50, 100 and 200 metres perpendicular to the road in both directions. Samples were also taken at the centreline at 0.8 km increments to the NW of the primary site (Figure 2). In total 14 experiments were performed consisting of four 30 minute integrated periods providing a total of 56 experiments (Benson, 1989).

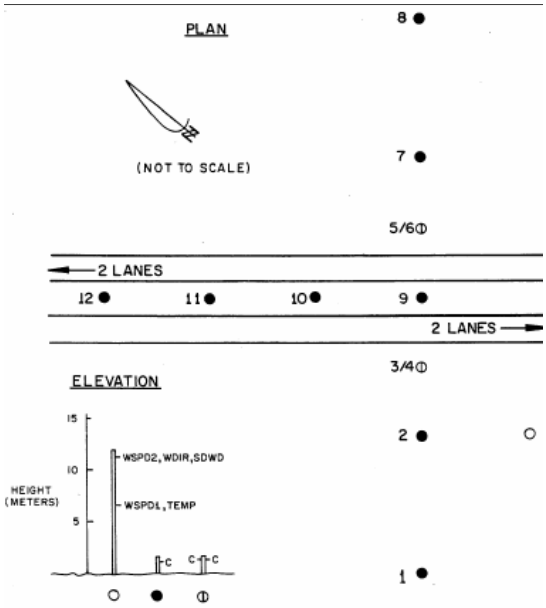

Figure 2. Schematic diagram of Caltrans 99 sampling locations- filled and unfilled dots (Benson, 1989). Road geometry is also shown.

3.2. Results and Discussion

Table 1 provides a subset of performance statistics for the LWM and Caline-4 models. Results are given for each horizontal and vertical diffusion option of LWM (which used the modified Caline-4 algorithm for initial mixing in all cases). Results are also provided for Caline-4 using actual site geometry i.e. 4 lanes, or for a surrogate of 2 lanes centred in the middle of the north and south bound lanes or as 1 lane centred on the median strip. Both the LWM and Caline-4 models were run with the measured 30 minute average meteorology and an assumed roughness of 0.1 m as the surrounding area is described as open fields with scattered residential development (Benson, 1989). Values of u^*, L and Z_i, were derived from the meteorological observations (wind speed at two heights, temperature at one height, wind direction fluctuation and a derived stability class).

Table1. Selected statistics for LWM and Caline-4.

	Average		**Stdev**		**Cor**	**Fa2**
	Unfiltered data					
	Obs	*Mod*	*Obs*	*Mod*	*Mod*	*Mod*
A	1057	1285	1023	1510	0.64	0.40
B	1057	1348	1023	1627	0.64	0.40
C	1057	1250	1023	1459	0.63	0.39
D	1057	996	1023	1108	0.80	0.47
E	1057	1111	1023	1545	0.68	0.46
F	1057	988	1023	1129	0.78	0.45
C1	1057	995	1023	1343	0.82	0.35
C2	1057	567	1023	614	0.85	0.19
C4	1057	612	1023	667	0.84	0.22
Data filtered upwind and for values less than 10 ppt						
A	1431	1834	972	1483	0.46	0.56
B	1431	1905	972	1620	0.48	0.55
C	1431	1710	972	1450	0.48	0.53
D	1431	1424	972	1061	0.69	0.66
E	1431	1563	972	1601	0.58	0.64
F	1431	1352	972	1113	0.69	0.63
C1	1431	1411	972	1397	0.76	0.48
C2	1431	801	972	586	0.78	0.25
C4	1431	865	972	639	0.76	0.29

A: Horizontal = σ_y, Vertical = Hysplit
B: Horizontal = σ_θ, Vertical = Hysplit
C: Horizontal = similarity, Vertical = Hysplit
D: Horizontal = σ_y, Vertical = modified Hysplit
E: Horizontal = σ_θ, Vertical = modified Hysplit
F: Horizontal = similarity, Vertical = modified Hysplit
C1: Caline-4 with 1 lane geometry
C2: Caline-4 with 2 lane geometry
C4: Caline-4 with 4 lane geometry
Cor=Correlation coefficient, Fa2= Factor of two

The results in Table 1 indicate that the LWM has comparable or better performance than Caline-4. Indeed when operating with the actual site geometry, the LWM performs better in all modes compared to the Caline-4 model. It is also evident that the LWM has superior performance when utilising the σ_z surface layer modified Hysplit vertical dispersion routine. The scatter plots shown in Figures 3 and 4 display performance data that has been filtered to remove upwind concentrations (see discussion below) and concentrations of 10 ppt or smaller. In these plots both Caline-4 and LWM are seen to over predict on some occasions. The vast majority of the over predictions occur at the downwind sites (1, 2, 3/4, 5/6, 7, 8 in Figure 2) for cases that include a very light and variable wind or for light winds with directions which are close to parallel with the road. In these cases the results are highly sensitive to the reported wind direction. Whilst not dismissing the observational data, it should be noted that a number of the reported concentrations are difficult to reconcile and impossible to achieve when modelling with constant meteorology. Consider for instance Figure 5 which displays data for one of the 14 days. The figure displays a wind direction arrow and scaled dots representing concentrations measured at the observational sites. Clearly there are a number of concentration observations that do not intuitively match the given meteorology. Whilst the winds appear relatively steady with a low to moderate meander, the observed concentrations clearly show a residual component in the third (C) and fourth (D) time periods north of the road. The results are improved by filtering the data to remove upwind components (see Table 1), but are still prone to error for the downwind sites in these instances.

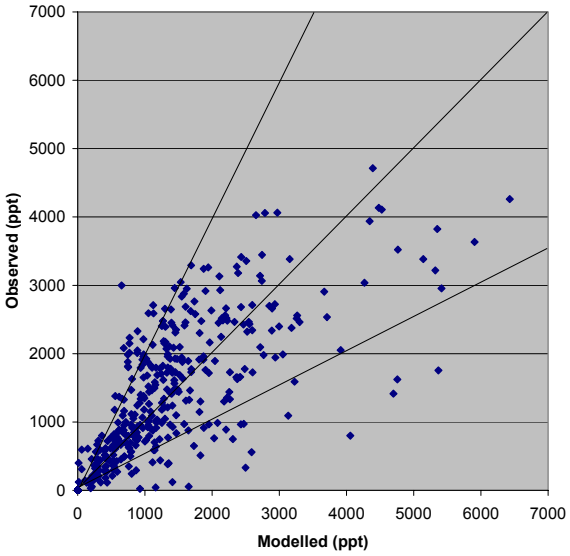

Figure 3: LWM scatter plot using the modified caline-4 mixing model, σ_y based horizontal diffusion and a σ_z modified Hysplit algorithm (Case D in Table 1).

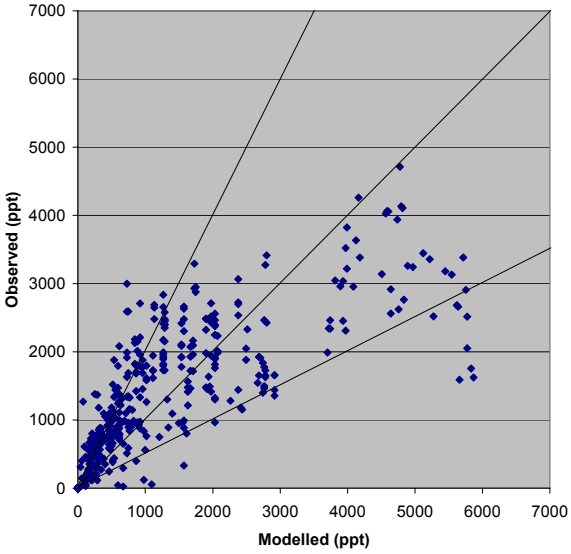

Figure 4: Caline-4 scatter plot using 1 lane geometry (Case C1 in Table 1).

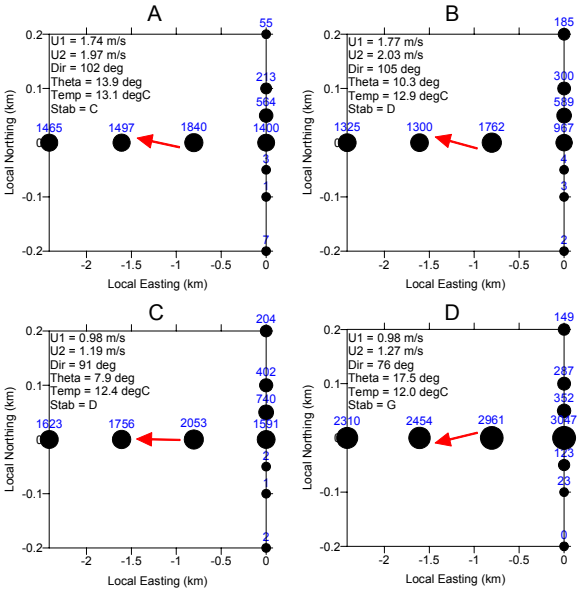

Figure 5: Concentration profiles for case 03-02-1982. Note the reported wind direction has been altered to match a reorientation of the roadway to an E-W direction. For each 30 minute period (A to D), the red arrows represent the average wind direction, the values in blue present the average concentration (ppb) which are represented visually by the size of the black markers.

3.3. Conclusions

A new chemically reactive plume dispersion model (LWM) has been developed and tested against a tracer validation suite and compared with Caline-4. The results are encouraging with the LWM results equal to or better than those obtained from Caline-4 for the case of an inert tracer, whilst the model allows the extra functionality of improved chemical transformation, simultaneous interaction of all source types and direct coupling with the advanced Eulerian model, TAPM.

Acknowledgments

The authors gratefully acknowledge the support of the CSIRO Energy Transformed Flagship.

References

Alderman, Z. (1999). A re-evaluation of the Carbon Bond-IV photochemical mechanism. Masters of Science Thesis, Dept of Env. Science and Eng, University of North Carolina, US. pp208.

Azzi, M., Johnson, G.M., and Cope, M. (1992). 'An introduction to the generic reaction set photochemical smog mechanism', *Proc of the 11th Int. Clean Air and Env. Conf.*, Brisbane, 1992, CASANZ.

Benson, P.E. (1989). *CALINE-4. A dispersion model for predicting air pollutant concentrations near roadways.* Final Report, FHWA/CA/TL84/15.

California Department of Transportation, Sacramento, CA.

Briggs, G.A. (1975). Plume rise predictions, in *Lectures of Air Pollution and Environmental Impact Analyses*, Workshop proceedings, Boston, Mass. Sep29–Oct3, 1975. pp 59-111, American Met. Society, Boston, Mass.

Draxler, R. and Hess. G. (2004). *Description of the Hysplit-4 modelling system.* Air Resources Laboratory, Silver Spring, Maryland, pp1-28

Held, T., Chang, D.P.Y. and Niemeier, D.A. (2003). UCD2001: An improved model to simulate pollutant dispersion from roadways. *Atmospheric Environment*, 37, 5325-5336.

Hurley, P. (2002). *The Air Pollution Model (TAPM) Version 2. Part 1: Technical Description*. CSIRO Atmospheric Research, Aspendale, Vic, Australia.

McRae, G. J., Goodin, W.R. and Seinfeld, J.H. (1982). Numerical solution of the atmospheric diffusion equation for chemically reactive flows. *Journal of Computational Physics, 45, 1-42.*

Nyugen, N., Lilley, W.E. and Williams, D.J. (2000). Development of a technique for estimating traffic emission and fuel consumption from SCATS road networks. *Proc of the 15th Int. Clean Air and Env. Conf., Sydney, 2000*, CASANZ.

Rao, K.S. (2002). Roadway-2: A model for pollutant dispersion near roadways, *Water, Air and Soil Pollution: Focus 2:* 261-277.

Seinfeld, J.H. and Pandis, S.N. (1998). *Atmospheric chemistry and physics: From air pollution to climate change.* Wiley Interscience, pp 1326.

Sharma, P. and Khare, M. (2001). Modelling of vehicular exhausts – a review. *Transport Research Part D6*. p179-198.